

Research Article

Texture Control During the Manufacturing of Nonoriented Electrical Steels

Leo Kestens¹ and Sigrid Jacobs²

¹ Department of Materials Science and Engineering, Delft University of Technology, Mekelweg 2, 2628 CD Delft, The Netherlands

² Electrical Steel Product Development Management, ArcelorMittal, Guldensporenpark 78, 9820 Merelbeke, Belgium

Correspondence should be addressed to Leo Kestens, l.a.i.kestens@tnw.tudelft.nl

Received 20 July 2007; Accepted 19 February 2008

Recommended by Claude Esling

Methods of modern quantitative texture analysis are applied in order to characterize the crystallographic texture of various non-oriented electrical steel grades in view of their relation with the magnetic properties of the steel sheet. A texture parameter is defined which quantifies the density of $\langle 100 \rangle$ easy magnetic directions in the sheet planes. An extensive correlation study revealed the relation of this parameter with the hysteresis losses, determined at an induction of 1.5 T, and with the induction measured at an applied external field of 25 A/cm. It is shown that the latter magnetic property is the more texture dependent, whereas the former one is more sensitive to the grain size of the steel. Also various strategies for texture control are critically reviewed. It is shown that the conventional manufacturing process only provides poor tools for optimizing the texture of the final product. In order to obtain a quantum-leap improvement of the magnetic quality of the texture, in combination with other important microstructural features, nonstandard processing strategies are required, such as cross-rolling, two-stage cold rolling, or surface annealing.

Copyright © 2008 L. Kestens and S. Jacobs. This is an open access article distributed under the Creative Commons Attribution License, which permits unrestricted use, distribution, and reproduction in any medium, provided the original work is properly cited.

1. INTRODUCTION

As finished products, industrially manufactured nonoriented electrical steels are single-phase ferrite polycrystalline materials. A macroscopic volume of such a material contains an aggregate of a large number of microscopically small granular crystallites. Each of the individual grains in the polycrystalline aggregate displays a specific orientation with respect to an external reference frame. In general, these grains are not randomly oriented, but a preference for certain orientations may be present. In this case, the material exhibits a specific crystallographic texture. On the other hand, when the grains are oriented in an arbitrary manner, the material is textureless or displays a random texture.

Each individual crystal orientation is characterized by the orientation relation between the sample and the crystal reference frame. The sample reference frame is a right-handed orthonormal (x^s, y^s, z^s) coordinate system which coincides with the RD, TD, and ND directions of the rolled sheet (rolling, transverse, and normal direction, resp.). The crystal reference frame is also a right-handed orthonormal

coordinate system which is attached to the $\langle 100 \rangle$ directions of the cubic crystal lattice. The orientation relation between crystal and sample reference system is uniquely determined by the three Euler angles $\varphi_1, \Phi, \varphi_2$. These angles define three consecutive rotations which must be carried out according to the schedule of Figure 1 in which the Bunge convention is adopted [1]. By executing these three rotations, the sample reference system is brought to coincidence with the crystal reference system.

For each of the grains present in the polycrystalline material, its orientation can be uniquely specified by means of these three Euler angles. Each set of three Euler angles $(\varphi_1, \Phi, \varphi_2)$ determines the coordinate of a point in the orientation space which is defined in the usual Euclidean way by the three orthogonal axes corresponding to the three Euler angles, (cf., Figure 2). Imagine that for each volume element of a material, it would be possible to determine precisely its crystallographic orientation. Then, each volume element would be represented by a specific point in Euler space (cf., Figure 2). In case that the material displays a certain texture, these representation points exhibit a specific

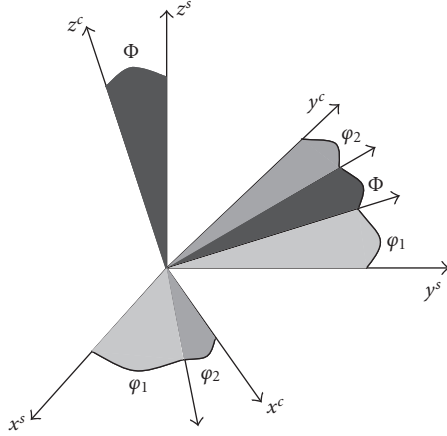


FIGURE 1: Definition of the Euler angles according to the Bunge notations. The set of three Euler angles $(\varphi_1, \Phi, \varphi_2)$ uniquely determines the correspondence between the sample reference (x^s, y^s, z^s) and the crystal reference frame (x^c, y^c, z^c) .

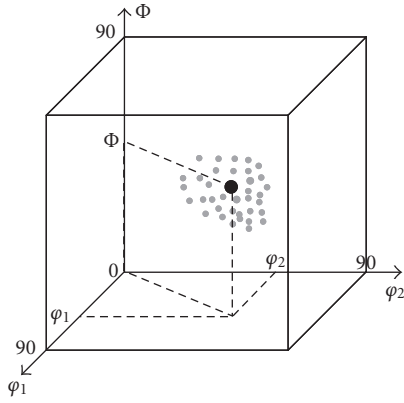


FIGURE 2: Representation of individual orientations in Euler space jointly representing a specific distribution which characterizes the crystallographic texture of the material.

distribution which characterizes the *orientation distribution function* (ODF):

$$f(g)dg = \frac{dV}{V} \quad (1)$$

with dV/V = the volume fraction of material represented by an infinitesimal orientation element dg around an arbitrary orientation g . This ODF is a three-dimensional distribution function which contains the entire texture information of the material under consideration.

Due to intrinsic symmetry properties of rolled sheet material such as nonoriented (NO) electrical steels, the domain of the ODF can be restricted to the following subspace $0 < (\varphi_1, \Phi, \varphi_2) < 90$ deg. Moreover, due to a fortunate coincidence, almost all texture components which are observed in cold rolled or annealed sheet steel are represented in the $\varphi_2 = 45$ deg section of Euler space. There-

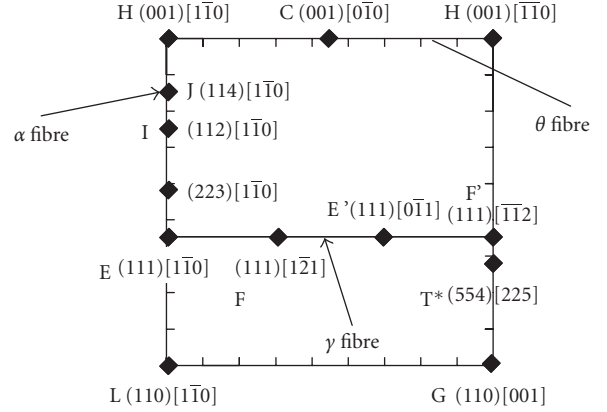


FIGURE 3: Characteristic $\varphi_2 = 45$ deg section of Euler space which represents the most common rolling and recrystallization components of low-carbon steels. The α , γ , and θ fibres represent groups of orientations for which $\langle 110 \rangle // RD$, $\langle 111 \rangle // ND$, and $\langle 001 \rangle // ND$, respectively. C = cube $\{001\} \langle 100 \rangle$, H = rotated cube $\{001\} \langle 110 \rangle$, G = Goss component $\{110\} \langle 001 \rangle$.

fore, the ODF of a low-carbon steel sheet is most commonly depicted by this section only. Figure 3 shows the characteristic texture components which are represented in the $\varphi_2 = 45$ deg section. They are mainly the cube ($\{001\} \langle 001 \rangle$), the rotated cube ($\{001\} \langle 110 \rangle$), and the Goss ($\{110\} \langle 001 \rangle$) components which are of importance for magnetic applications. Apart from individual texture components also fibre components are displayed. These fibre components represent a group of orientations for which one crystal direction corresponds to a specific sample direction. The most important fibres are the α , γ , and θ fibres for which $\langle 110 \rangle // RD$, $\langle 111 \rangle // ND$, and $\langle 001 \rangle // ND$, respectively.

2. EVALUATION OF THE MAGNETIC QUALITY OF A TEXTURE

When one wants to investigate the effect of texture on the magnetic properties of electrical steel, reliable quantitative parameters are required to characterize both the dependent and the independent variables, that is, magnetic properties and texture, respectively. With regard to the magnetic properties, the usual quantitative features can be employed such as the core losses, the permeability, the coercive field, the remnant induction, and other characteristics of the hysteresis curve. With regard to the texture, one must take into account the physical fact that the $\langle 100 \rangle$ directions are the directions of easy magnetization of a Fe-single crystal [2]. The Fe-single crystal magnetization curves show that optimum soft magnetic properties are obtained when the external field is applied in the $\langle 100 \rangle$ direction. Therefore, the ideal texture of a soft iron core is the one that maximizes the density of $\langle 100 \rangle$ crystal directions parallel to the flux lines of magnetic induction. Because in rotating applications the flux lines are nearly isotropically distributed in the laminated sheets, the ideal texture is the one that maximizes the incidence

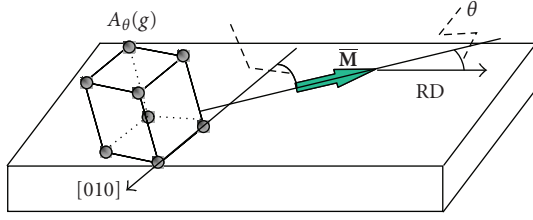


FIGURE 4: definition of the $A_\theta(g)$ parameter as the minimum angle between the direction of the magnetization vector \mathbf{M} and the nearest $\langle 100 \rangle$ direction of the crystal.

of $\langle 100 \rangle$ directions in the plane of the sheet. This is not the well-known Goss component ($\{110\}\langle 001 \rangle$) which is usually observed in grain-oriented steels [3], but rather the orientations of the cube fibre for which the $\{001\}$ planes are parallel to the rolling plane. The latter texture components display two coplanar $\langle 100 \rangle$ directions in the plane of the sheet, whereas the former component only delivers one $\langle 100 \rangle$ direction to the lamellar plane.

In order to quantify the magnetic quality of an arbitrary NO steel texture, a precise parameter is defined which can be derived from the ODF. For every arbitrary crystal orientation g , the angle $A(g)$ can be determined which is the minimum angle between the direction of the magnetization vector \mathbf{M} and the closest $\langle 100 \rangle$ direction (out of 3 symmetric equivalent $\langle 100 \rangle$ directions), compared to (cf., Figure 4). The texture parameter A_θ is defined as the orientation-averaged value of $A(g)$, taking into account the volume fraction of each texture component, for an arbitrary magnetic field direction θ . This orientation weighted average value can be very elegantly expressed by the convolution integral of $A_\theta(g)$ and the ODF $f(g)$,

$$A_\theta = \int f(g)A_\theta(g)dg. \quad (2)$$

The value of A_θ is confined to the range (0–54.7 deg). The lower limit corresponds to the case of a single component texture in which one of the $\langle 100 \rangle$ directions of the crystal lattice corresponds to the magnetization direction, whereas the upper limit is observed for a single component texture in which the direction of magnetization is aligned with the $\langle 111 \rangle$ lattice direction.

In rotating electrical machine applications, the directions of the magnetizing field will be equally distributed in the lamellar plane of the rolled sheet. Consequently, a direction averaged A parameter must be considered as

$$A = \int A_\theta d\theta, \quad (3)$$

in which the integral expands over all possible planar directions of the rolled sheet. For a sample with orthorhombic sample symmetry, as usually observed in cold-rolled sheet steel, the integral of (3) can be readily approximated by the following expression:

$$A = \frac{A_0 + 2A_{45} + A_{90}}{4}, \quad (4)$$

TABLE 1: Direction-averaged A values (in deg) of a number of texture components and fibres which are present in the typical texture of NO electrical steels (random refers to a random texture).

$\{001\}\langle 110 \rangle$	θ fibre	α fibre	γ fibre
22.5	22.5	30.1	38.7
$\{110\}\langle 001 \rangle$	$\{001\}\langle 001 \rangle$	$\{112\}\langle 110 \rangle$	random
33.8	22.5	36.1	31.9

in which A_0 , A_{45} , and A_{90} represent the A values (according to (2)) for an applied field which encloses an angle of 0, 45, and 90 deg, respectively, with the direction of rolling.

A low value of the A parameter corresponds to a high magnetic quality of the texture because it implies that, on average, the $\langle 100 \rangle$ directions are closely aligned with the flux lines which are randomly distributed in the plane of the sheet. Table 1 presents the direction averaged (according to (4)) A parameters for a number of ideal texture components. It can be demonstrated that the theoretically lowest value of the A parameter is 22.5 deg. According to the data of Table 1, this value is displayed by all individual components of the θ fibre, and also by the θ fibre itself. Therefore, the above presumption is vindicated, that is, the cube fibre (θ fibre) is truly the ideal texture for NO electrical steels. This conclusion was reported as well by Rollett et al. [4].

3. CORRELATION BETWEEN TEXTURE AND MAGNETIC PROPERTIES

Once a reliable procedure has been established to quantify both the texture and the magnetic properties, a relation between them can be investigated. Such a correlation study can only be carried out successfully on condition that the independent variable (i.e., the crystallographic texture characterized by its A value) can be varied over a sufficiently wide range in order to gauge the effect on the dependent variable. In order to achieve this goal a dedicated data set was produced composed of a number of samples for which the A_θ parameters varied between 27.7 and 36.3 deg. For each of these samples belonging to the data set, the hysteresis losses were measured for a magnetic induction of 1.5 T and the permeability was assessed by measuring the magnetic induction for an applied magnetic field of 25 A/cm. All these magnetic properties were measured at 0, 45, and 90 deg with respect to the rolling direction and correlated with A_0 , A_{45} , and A_{90} , respectively.

The metallurgical methods employed to produce samples with varying textures had also introduced a considerable spread of grain size in the dataset. Because grain size may also have an important effect on the magnetic properties, this parameter had to be included in the correlation study as well. The linear regression equations which correlate the A value and the average grain diameter D with the magnetic

properties (P_h at 1.5 T and B25) reveal the following correspondences:

$$P_h = (-3.9 \pm 0.8)D + (0.15 \pm 0.04)A - 0.869, \quad (5)$$

with $r^2 = 0.632$,

$$B25 = (-0.016 \pm 0.04)A + 2.164, \quad \text{with } r^2 = 0.848. \quad (6)$$

In the above equations, the hysteresis loss is expressed in W/kg, the induction B25 in T, the A parameter in hexadecimal degrees and the grain size D in mm. Because the grain size only had a minor effect on the induction, the parameter D could be ignored in the regression equation (6).

In order to estimate the texture effect, the following comparison can be considered. If the texture could be controlled in the most ideal way such that the theoretically optimum A parameter could be achieved of 22.5 deg, it would imply a drop of approximately 10 deg compared to the A value of 32 deg which is regularly observed on industrially manufactured NO steels (cf., infra). The above regression equations (5) and (6) show that such a 10 deg drop of the A value will produce a decrease of 1.5 W/kg in hysteresis losses and an increase of induction (B25) with 160 mT. These values must be compared with the changes that can be produced by other independent state variables of the microstructure such as grain size, precipitation density, or residual stresses. When such a critical analysis is carried out, it can be concluded that the texture has its most significant effect on the induction B25, which in this study is used as a measure for the permeability. With regard to the hysteresis P_h losses at 1.5 T, the grain size is much more decisive than the texture. The relative lack of correlation with a regression coefficient of $r^2 = 0.632$ indicates that also other microstructural features which were not taken into account here such as, for example, residual stresses or presence of precipitates may affect the hysteresis losses.

On the theoretical level, it could be argued that the induction B25 measured at an applied field of 25 A/cm is not the most sensitive magnetic parameter to reflect the influence of texture neither. In the magnetization curve, two different parts can be distinguished: the lower part (below the characteristic deflection point) which is controlled by magnetic domain wall displacement and the upper part (above the characteristic deflection point) which is controlled by rotational magnetization. It is the latter part which is the most dependent on the texture. This part of the magnetization curve can be appropriately characterized by the difference in saturation induction B_{sat} and remnant induction B_{rem} . Therefore, in spite of the practical problems in determining the exact B_{sat} value experimentally, in order to further examine the effect of texture on the magnetic behavior of NO electrical steels, it is suggested to use this difference ($B_{\text{sat}} - B_{\text{rem}}$) as the reference magnetic parameter.

4. CONVENTIONAL TEXTURE CONTROL IN NO ELECTRICAL STEELS

On the basis of an extensive testing program on industrially manufactured NO steel grades, it was concluded that even

the widest variation of conventional processing parameters applied in state-of-the-art steel manufacturing would only produce limited variations in the magnetic quality of the textures. In these experiments, the following processing parameters were considered: slab reheating temperature (SRT), finish rolling temperature (FRT), hot band coiling temperature (CT), hot band annealing (yes/no), cold rolling reduction (CR), continuous annealing temperature, line speed of continuous annealing, and skin pass reduction (SKP). On top of this, also the chemical composition of these steel was thoroughly investigated. The applied windows for all these processing and chemical parameters are listed in Table 2. Despite these wide scale variations, the A_0 parameter only varied between 25 and 31 deg, whereas theoretically this value can change between 0 and 55 deg.

Figure 5 displays the typical ODFs which are observed in the subsequent stages of the manufacturing process of NO electrical steels. The textures reported in Figure 5 are measured in the middle of the sheet and thus represent the bulk textures. The single most important processing factor for texture control is the finish rolling temperature (FRT). Whereas for structural steels the conventional FRT is in the full austenite region [5], for NO electrical steels the optimum textures are obtained with finish rolling in the two-phase region or even the full ferrite phase. Figure 5(a) displays the hot band texture which is observed after such a two-phase rolling. It is characterized by a very strong maximum on the rotated cube component (with an intensity maximum of $>30x$) and an extension along the α fibre toward the $\{112\}\langle 110 \rangle$ component. After a typical cold rolling reduction of 70%, the intensity is more homogeneously spread along the α fibre, but a maximum of $>20x$ still remains on the rotated cube component (cf., Figure 5(b)). The rotation flow as a result of cold deformation can be entirely understood on the basis of the classical full constraints Taylor theory and its relaxed constraints derivatives [6].

After primary recrystallization, the texture is significantly weakened as compared to the hot band and the cold rolling textures (cf., Figure 5(c)). Although the intensity maximum remains on the rotated cube component ($\{001\}\langle 110 \rangle$), it has decreased from $>20x$ to $\sim 5x$. The metallurgical mechanisms that controlled the recrystallization of the cold-rolled sheet did not allow the magnetically favorable $\{001\}$ orientations, which dominated the hot and cold band textures, to be preserved in the annealing texture. Conversely, as shown in Figure 5(c), the recrystallization of a 70% cold-rolled product will rather favor the $\{111\}$ orientations at the expense of the $\{001\}$ orientations [7]. In principle, for the type of low Si grade NO steels presently under consideration, the quality of both the hot band microstructure and texture is more favorable with regard to the magnetic properties than the quality of the cold-rolled and annealed product. In many instances, also the grain size of hot-rolled sheet and additional microstructural features such as density or morphology of 2nd phase particles is commonly appropriate in terms of magnetic quality. Unfortunately, the required gauges of 0.65 mm or less cannot be obtained on current state-of-the-art hot rolling mills and thus, a subsequent cold rolling and annealing stage is unavoidable.

TABLE 2: Variation range of the following steel manufacturing processing parameters: SRT = slab reheating temperature, FRT = finish rolling temperature, CT = hot band coiling temperature, line speed and annealing temperature of the continuous annealing line, and skin pass reduction. Also the minimum and maximum levels (in mass %) of various alloying elements are listed.

Process parameter	Min.	Max.	Element	Min.	Max.
SRT. (°C)	1070	1250	C	0.021	0.055
FRT (°C)	790	920	Si	0.000	2.153
CT (°C)	580	780	P	0.006	0.032
Hot band annealing	no	yes	S	0.008	0.033
Line speed (m/min)	150	250	N ₂	0.0017	0.0224
Annealing temp. (°C)	700	800	Al _{met}	0.011	1.060
Skin pass red. (%)	2	8	Sb	0.000	0.160

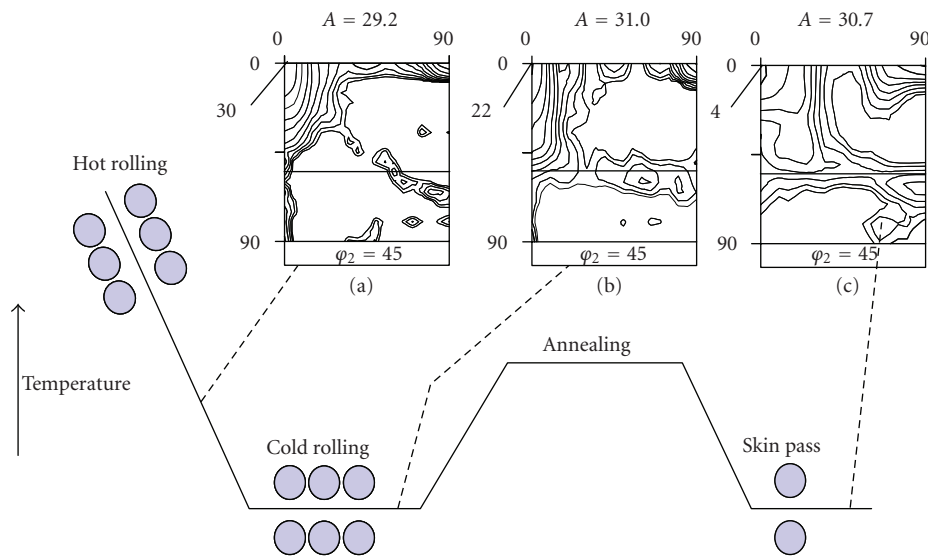


FIGURE 5: Typical texture evolution during the subsequent stages of the conventional manufacturing process of a fully processed NO electrical steel: (a) hot band texture, (b) cold rolling texture, and (c) annealing texture.

A substantial part of the volume of NO electrical steels is manufactured as semiprocessed sheet. These semiprocessed products are submitted to a skin pass reduction of 4 to 8% and additionally an annealing treatment is carried out on the punched laminations which are ready to be processed in soft-iron cores of electrical devices. This additional heat treatment, which is commonly carried out not by the steel manufacturer but by the manufacturer of iron cores, serves multiple purposes such as decarburization, grain growth, or relieving of internal stresses. This treatment definitely also affects the texture of the final product as it is exhibited in Figure 6. The ODF after this final annealing treatment displays two characteristic maxima: one on the α fibre in the vicinity of the $\{113\}\langle 110 \rangle$ component and one on the TD fibre ($\langle 110 \rangle // TD$) some 10 deg away from the Goss component. Although a marked textural change has occurred, the magnetic quality of the texture in terms of its average A value was hardly affected at all by the additional heat treatment on the stamped lamella. It was shown that

the texture which was produced by the annealing could be explained by considering the stored energy of plastic deformation after skin pass rolling [8].

5. ADDITIONAL METHODS OF TEXTURE CONTROL IN NO ELECTRICAL STEELS

5.1. Cross rolling

In order to control the recrystallization texture, one has to bear in mind that during the annealing of cold-rolled sheet a selection will be made of orientations which have developed during the cold rolling process. Therefore, it should be attempted to form as few as possible unfavorable orientations of the α and γ fibres as a result of the rolling strain. Unfortunately, these are the stable end orientations which appear after conventional rolling reductions of 60 to 80% [5]. By changing the orientations of the rolling-mill rolls with respect to the sheet, the rotation paths of the orientation flow

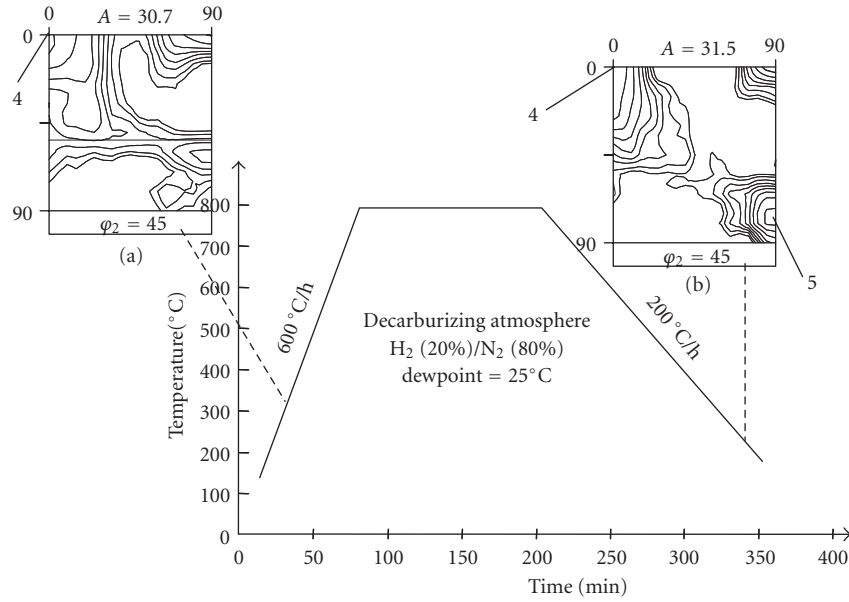


FIGURE 6: Texture evolution as a result of skin pass annealing (with decarburization) on a semiprocessed NO electrical steel: ODF (a) before and (b) after the annealing treatment.

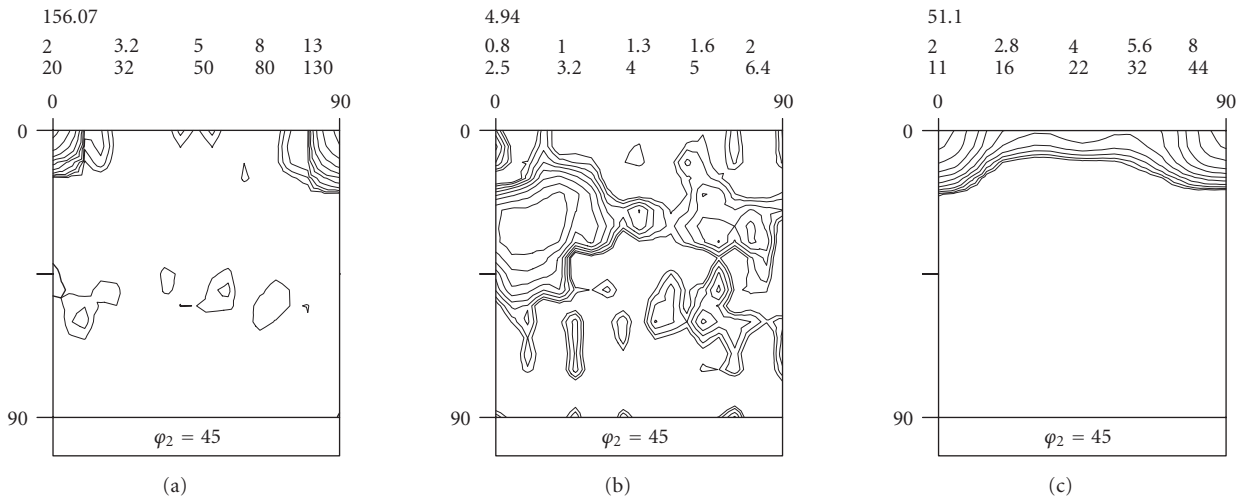


FIGURE 7: ODFs observed after cross rolling: (a) rolling texture, (b) primary recrystallization texture, and (c) after additional annealing treatment.

during plastic deformation can be affected. In the present study, a laboratory scale experiment was carried out in which the hot-rolled sheet was 90 deg rotated before cold rolling. In doing so the RD of hot rolling turns into the TD of cold rolling and vice versa. Hence, the hot band texture, with its characteristic strong α fibre (cf., Figure 5(a)) is transformed into a texture with a strong $\{110\}$ //TD fibre by simply substituting the hot rolling by the cold rolling reference frame. Because the latter fibre is highly unstable for cold rolling, all its components will rotate toward the semistable $\{001\}\langle 110 \rangle$ orientation. This procedure will give rise to

an extremely strong rotated cube component ($\{001\}\langle 110 \rangle$) with an extraordinary intensity of $>150\times$, compared to Figure 7(a), which offers the advantage that it does not introduce the unfavorable α and γ fibre components during cold reduction. This favorable texture is not preserved, though, after the primary recrystallization treatment which produces a rather weak texture with a maximum in the vicinity of $\{112\}\langle 110 \rangle$ (cf., Figure 7(b)).

When this material is cold rolled to a reduction of 4 to 8% and submitted to an additional annealing treatment, comparable to the one which is applied to semiprocessed

products, the rotated cube component spectacularly reappears in the material and even other components of the θ fibre are formed. The texture presented in Figure 7(c) is the result of such an additional annealing treatment. It displays a maximum of $>50\times$ on the rotated cube component and $\sim 10\times$ on the cube component. The exceptional magnetic quality of this texture is reflected in the very low average A value of 24.3 deg which is only 1.8 deg away from the theoretical minimum value of 22.5 deg. It is obvious that cross rolling cannot be implemented in a continuous line manufacturing process. Whether or not the proposed process with cross rolling is of industrial relevance is entirely dependent of economic considerations, that is, added economic value by superior material properties versus increased manufacturing cost because of loss of production efficiency.

5.2. Two-stage cold rolling

Conventional continuous annealing is applied on a cold-rolled material with a rolling strain of 70% reduction at a temperature between 700 and 850°C and with a heating rate of 2 to 10°C/s. These large rolling reductions are necessary to obtain the relatively thin gauges of 0.60 mm or less which are generally required for the production of soft iron core lamella. The metallurgical mechanisms, however, which control the texture formation during recrystallization under these circumstances only favor the nucleation of $\{111\}$ orientations which are highly unfavorable for magnetic purposes. Other recrystallization mechanisms which stimulate the formation of the desired $\{001\}$ orientations only operate after limited rolling strains (of the order $<10\%$). Therefore, it is an interesting strategy to apply the necessary reduction in two stages: at first a substantial reduction (60 to 70%) in order to obtain the required gauge followed by a second much lower reduction (5 to 10%) in order to control the texture and the microstructure. This production path can be associated with the manufacturing of semiprocessed grades of NO steels which are produced by a similar approach. It is known that the magnetic quality of the texture may largely benefit from an annealing treatment carried out on a temper-rolled material [9–12].

The magnetic properties, measured on a 0.65 mm gauge sheet, of two NO steels are compared in Table 3. One NO steel was cold manufactured in a one stage process, whereas the other one was produced in a two-stage process. The first column pertains to a set of samples that were cold rolled in one stage with a reduction of 70%, whereas the second column refers to the samples which were submitted to an intermediate annealing treatment between two successive rolling operations with a reduction of 70 and 10.4%, respectively. After the second rolling, a final annealing treatment was applied. It can be noticed that primarily the hysteresis losses are favorably affected by this process, whereas the B25 and B50 values are hardly affected at all.

The reason for this behavior must be explained in terms of the microstructural and textural evolution. The annealing treatment following a small rolling strain triggers a process of strain-induced abnormal grain growth [13] which is highly beneficial for the hysteresis losses. Although this grain

TABLE 3: Comparison of the magnetic properties of two sets of samples. One set is cold rolled in a single stage with a reduction of 70% and the other set was intermediately annealed between cold rolling stages with a reduction of 70 and 10.4%, respectively, prior to a final annealing treatment.

Property	Sample	
	One-stage cold rolling	Two-stage cold rolling
$P(1.5)$ [W/kg]	6.61	5.14
$P_h(1.5)$ [W/kg]	3.80	2.28
$P_w(1.5)$ [W/kg]	2.81	2.86
$P(1)$ [W/kg]	3.09	2.34
B25 [T]	1.65	1.65
B50 [T]	1.74	1.73
A-parameter (deg) (direction averaged)	30.9	31.8

growth process is also accompanied by a marked texture evolution, the A parameter change (cf., Table 3) indicates that the magnetic quality of the texture has not improved. The reason for this behavior is complex and is not entirely understood as yet, but it is related with the detailed features of the recrystallization and grain growth mechanisms which operate after such low rolling reductions.

5.3. Surface textures

Yoshinaga et al. [14] have demonstrated that a relatively strong rotated cube texture can be obtained at the surface of an ultra-low-carbon steel when a conventionally cold-rolled sheet of this material is submitted to a short annealing treatment (2 to 3 minutes) in the full austenite phase. The forward and reverse ferrite to austenite transformation produces textures of the type presented in Figure 8. It can be observed that there is a pronounced difference between the surface and the bulk textures. It is assumed that the surface energy will drastically affect the orientation selection occurring during the diffusion-controlled phase transformation.

Once a favorable surface texture is created, a method must be established which allows the surface grains to grow into the bulk of the sheet. Such a method is part of the metallurgical process proposed by Tomida [15]. He performed a two-stage annealing treatment on a cold rolled and recrystallized NO electrical steel with a Mn content of 1.0 to 2.5 mass% and a C content of 0.05 to 0.10 mass%. The first stage of this annealing treatment was carried out under vacuum conditions ($P < 10^{-5}$ hPa) during 12 hours at varying temperatures between 850 and 1100°C. During this stage of the annealing treatment, the Mn gradually diffused out of the surface layers of the sheet. As Mn is a strong austenite stabilizing element, the removal of Mn from the surface layer locally triggered a ferrite transformation near the surface with a favorable $\{001\}$ texture, very much comparable to the one observed by Yoshinaga et al. [14].

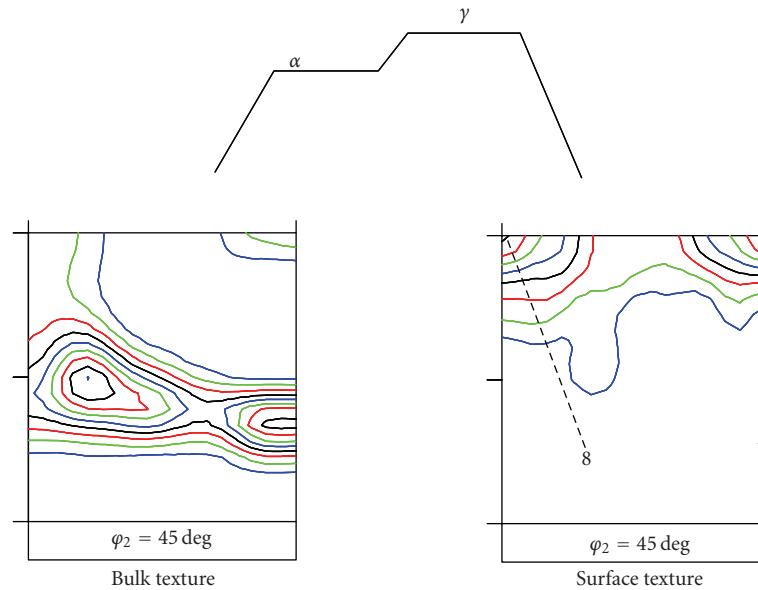


FIGURE 8: Textures observed after a forward and reverse ferrite-austenite transformation in an ultra-low-carbon steel (a) in the bulk and (b) at the surface of the sheet. Levels: 2-4-6-8-11-14 [14].

The second stage of the annealing treatment was carried out under a decarburizing atmosphere. Under these circumstances, the ferrite surface grains gradually consumed the austenite bulk of the material, hereby extending the favorable surface texture over the entire volume of the material and thus creating a columnar structure. By applying this method, extraordinary sharp cube textures could be produced concurrently with highly favorable columnar microstructures displaying an average grain size of more than $100\ \mu\text{m}$. This gave rise to a core loss between 1.4 and 1.7 W/kg and an induction of 1.76 to 1.81 T at an applied magnetic field of 50 A/cm.

6. SUMMARY AND CONCLUSIONS

In the present paper, the effect of texture on the magnetic properties of nonoriented electrical steels was analyzed. Based on the methods provided by modern quantitative texture analysis, a texture parameter was proposed which accurately characterizes the magnetic quality of any arbitrary steel texture. This parameter was correlated with a number of magnetic properties on an extensive set of steel samples. It was found that the texture has a larger impact on the permeability than on the core losses. The latter property is more dependent on the grain size than on the texture.

Various methods of texture control during steel manufacturing were evaluated. An extensive experimental study has revealed that the conventional processing parameters of a modern state-of-the-art steel plant only provide limited tools for an optimum texture control. It was shown that the finish temperature of hot rolling is the one single parameter of key importance for the development of a favorable magnetic texture on the final product after cold rolling and annealing.

In general, the comparatively favorable properties of the hot band texture and microstructure cannot be preserved after cold rolling and annealing. Therefore, nonconventional processing strategies were also investigated in the present study. A number of promising alternative techniques were evaluated such as cross rolling, two-stage cold rolling and surface annealing. In laboratory scale experiments, all of these techniques have proven to produce the favorable $\{001\}$ texture combined with optimum microstructural features favoring highly advantageous magnetic properties through a modification of the hysteresis loss.

ACKNOWLEDGMENT

The authors would like to acknowledge Mr. Ch. Standaert from the ArcelorMittal group for his collaboration in this study.

REFERENCES

- [1] H.-J. Bunge, *Texture Analysis in Materials Science: Mathematical Models*, Butterworths, London, UK, 1982.
- [2] C. W. Chen, *Magnetism and Metallurgy of Soft Magnetic Materials*, North-Holland, Amsterdam, The Netherlands, 1977.
- [3] J. Harase, R. Shimizu, and N. Takahashi, "Mechanism of Goss secondary recrystallization in grain-oriented silicon steel," *Textures and Microstructures*, vol. 14, part 3-4, pp. 679–684, 1991.
- [4] A. D. Rollett, M. L. Storch, E. J. Hilinski, and S. R. Goodman, "Approach to saturation in textured soft magnetic materials," *Metallurgical and Materials Transactions A*, vol. 32, no. 10, pp. 2595–2603, 2001.
- [5] L. Kestens and J. J. Jonas, "Transformation and recrystallization textures associated with steel processing," in *Metalworking: Bulk Forming*, S. L. Semiatin, Ed., vol. 14A of ASM

- Handbook*, pp. 685–700, ASM International, Materials Park, Ohio, USA, 2005.
- [6] P. Van Houtte, S. Li, M. Seefeldt, and L. Delannay, “Deformation texture prediction: from the Taylor model to the advanced Lamel model,” *International Journal of Plasticity*, vol. 21, no. 3, pp. 589–624, 2005.
- [7] K. Verbeken, L. Kestens, and J. J. Jonas, “Microtextural study of orientation change during nucleation and growth in a cold rolled ULC steel,” *Scripta Materialia*, vol. 48, no. 10, pp. 1457–1462, 2003.
- [8] L. Kestens, J. J. Jonas, P. Van Houtte, and E. Aernoudt, “Orientation selective recrystallization of nonoriented electrical steels,” *Metallurgical and Materials Transactions A*, vol. 27, no. 8, pp. 2347–2358, 1996.
- [9] J. P. Anderson and B. A. Lauer, “Electrical steel with improved magnetic properties in the rolling direction,” US patent no. 6,569,265, May 2003.
- [10] T. Shimazu, M. Shiozaki, and K. Kawasaki, “Effect of temper rolling on texture formation of semi-processed non-oriented steel,” *Journal of Magnetism and Magnetic Materials*, vol. 133, no. 1–3, pp. 147–149, 1994.
- [11] S. W. Cheong, E. J. Hilinski, and A. D. Rollett, “Effect of temper rolling on texture formation in a low loss cold-rolled magnetic lamination steel,” *Metallurgical and Materials Transactions A*, vol. 34, no. 6, pp. 1311–1319, 2003.
- [12] E. J. Hilinski, “Recent developments in semiprocessed cold rolled magnetic lamination steel,” *Journal of Magnetism and Magnetic Materials*, vol. 304, no. 2, pp. 172–177, 2006.
- [13] V. Randle, “Microtexture investigation of the relationship between strain and anomalous grain growth,” *Philosophical Magazine A*, vol. 67, no. 6, pp. 1301–1313, 1993.
- [14] N. Yoshinaga, L. Kestens, and B. C. De Cooman, “ $\alpha \rightarrow \gamma \rightarrow \alpha$ transformation texture formation at cold-rolled ultra low carbon steel surfaces,” *Materials Science Forum*, vol. 495–497, part 1–2, pp. 1267–1272, 2005.
- [15] T. Tomida, “A new process to develop (100) texture in silicon steel sheets,” *Journal of Materials Engineering and Performance*, vol. 5, no. 3, pp. 316–322, 1996.